

## EXAFS study of crystal structures of $(\text{Ba}_{1-x}\text{La}_x)_2\text{In}_2\text{O}_{5+x}$ and their oxide ion conductivity

Yoshiharu Uchimoto <sup>\* a</sup>, Hiromitsu Takagi <sup>a</sup>, Takeshi Yao <sup>a</sup>, Naoshi Ozawa <sup>a</sup>, Toru Inagaki <sup>b</sup>, and Hiroyuki Yoshida <sup>b</sup>

<sup>a</sup> Department of Fundamental Energy Science, Graduate School of Energy Science, Kyoto University, Yoshida, Sakyo-ku, Kyoto 606-8501, Japan, <sup>b</sup> Technical Research Center, The Kansai Electric Power Company, Inc., Amagasaki, Hyogo-ken 661-0974, Japan, \* Present address: Department of Applied Chemistry, Graduate School of Science and Engineering, Tokyo Institute of Technology, Ookayama, Meguro, Tokyo 152-8552, Japan. E-mail: [yuchimot@o.cc.titech.ac.jp](mailto:yuchimot@o.cc.titech.ac.jp)

Crystal structures of  $(\text{Ba}_{1-x}\text{La}_x)_2\text{In}_2\text{O}_{5+x}$  ( $x=0.00, 0.20, 0.30, 0.40, 0.50$ ) were analyzed by EXAFS and the powder X-ray Rietveld method. A Fourier transform of In K-edge EXAFS data from  $(\text{Ba}_{1-x}\text{La}_x)_2\text{In}_2\text{O}_{5+x}$  showed a peak between 1.2 and 2.0 Å attributed to the nearest oxide ions around  $\text{In}^{3+}$  cation. The peak was back-Fourier transformed, and the structural parameters were refined by the least square fitting. The coordination number of  $\text{In}^{3+}$  cation increases with increasing  $\text{La}^{3+}$  cation content. This means oxygen is introduced at interstitial site by keeping an electroneutrality. As a result of the oxygen distribution, the oxide ion vacancies distribute randomly. The electrical conductivities of  $(\text{Ba}_{1-x}\text{La}_x)_2\text{In}_2\text{O}_5$  rapidly increased above 1203 K due to the order-disorder transition of oxygen vacancy. On the other hand, the electrical conductivities of  $(\text{Ba}_{1-x}\text{La}_x)_2\text{In}_2\text{O}_{5+x}$  ( $x=0.20, 0.30, 0.35, 0.40, 0.45, 0.50$ ) did not show the sharp discontinuity in the conductivity because the disorder phase of defective perovskite type structure was stabilized by doping  $\text{La}^{3+}$  cations at A-site even at low temperature.

**Keywords:** EXAFS, coordination number, perovskite structure

### 1. Introduction

Recently, a significant amount of work has been devoted to solid oxide fuel cells (SOFCs) utilizing oxide ion conductors as electrolyte (Appleby *et al.*, 1989; Minh *et al.*, 1995). When the operating temperature is reduced to intermediate-temperature range (1000-1100 K), SOFCs could be constructed by less costly materials for interconnectors, for example alloys, and technical advantages such as increase a reliability and lifetime will be attained. Since oxide ion conductivity of stabilized zirconia decreases at such temperatures, some of the major problems found in the SOFCs can be attributed to difficulties in lowering the resistance of the oxide ion conductors. This can be achieved by increasing the specific ionic conductivity of the oxide ion conductor.

Oxides with perovskite and perovskite-related structures have been widely investigated for the electrolyte material for the SOFCs at the intermediate-temperature range (Ishihara *et al.*, 1994; Feng *et al.*, 1995; Goodenough *et al.*, 1990; Alder *et al.*, 1994; Zhang *et al.*, 1995). The defect perovskite-related oxide  $\text{Ba}_2\text{In}_2\text{O}_5$  has a characteristic order-disorder transition temperature ( $T_d$ ) at 1203 K, and has been reported to have high oxide ion conductivity, which is higher than that of calcia- and yttria-stabilized zirconia, at high temperature phase (Goodenough *et al.*,

1990; Alder *et al.*, 1994; Zhang *et al.*, 1995). In order to utilize as the electrolyte for SOFCs, It is important to stabilize the high temperature phase. We have attempted to stabilize the high temperature phases by La cation doping at A-site and discussed relationship of crystal structure of  $(\text{Ba}_{1-x}\text{La}_x)_2\text{In}_2\text{O}_{5+x}$  which was analyzed by powder X-ray Rietveld method and the oxide ion conductivity of the oxide (Uchimoto *et al.*, 2000). In this work, we have focused on the local structure change around In cations induced by the  $\text{La}^{3+}$  cation doping in order to clarify the relationship between the structural changes and the oxide ionic conductivity. The local structure of La-doped  $\text{Ba}_2\text{In}_2\text{O}_5$  was analyzed by EXAFS method. If the oxidation number of cations is fixed, e.g. oxidation number of Ba, In, La is 2+, 3+, 3+, respectively, with increase of La content oxygen coordination number increase.

### 2. Experimental

Pure and La doped  $\text{Ba}_2\text{In}_2\text{O}_5$  powder was prepared by usual solid-state reaction starting with Barium carbonate (Wako Chemical Co. Inc., 99.9%), indium oxide (Wako Chemical Co. Inc., 99.9%), and lanthanum oxide (Wako Chemical Co. Inc., 99.9%). The crystal structure of the product was determined by XRD using Mo-K $\alpha$  radiation. For the Rietveld analysis, a powder XRD pattern was collected using a Model RINT-TTR powder X-ray diffractometer (Rigaku Co.). The total electrical conductivity of the oxides is measured by impedance spectroscopy using impedance analyzer (Solatron 1260) connected with potentiostat (Solatron 1287). The ion-blocking technique is used to determine the oxide ion transference numbers.

The sample was ground to a fine powder and sandwiched between pieces of Scotch tape (3M Consumer Products Group, St. Paul, MN, USA). The EXAFS in the vicinity of In K-edge were measured on beam line BL01B1 at SPring-8 in Japan Synchrotron Radiation Research Institute. EXAFS analysis was conducted by using 'MELMS' computer program (Yao *et al.*, 1991; Yao, 1993).

### 3. Results and Discussion

XRD pattern of  $\text{Ba}_2\text{In}_2\text{O}_5$  was indexed to an orthorhombic lattice. On the other hand, XRD pattern of  $(\text{Ba}_{1-x}\text{La}_x)_2\text{In}_2\text{O}_{5+x}$  ( $X=0.20, 0.30, 0.40, 0.50$ ) was indexed to a cubic lattice (Uchimoto *et al.*, 2000). The lattice parameters and other structural parameters were refined by the Rietveld method and it was confirmed that the  $\text{Ba}_2\text{In}_2\text{O}_5$  belongs to orthorhombic *Ibm2* space group. (Uchimoto *et al.*, 1999) The  $\text{Ba}_2\text{In}_2\text{O}_5$  has Brownmillerite structure, which consists of the stacking of alternating two-dimensional layers of corner-shared  $\text{InO}_6$  octahedra and corner-shared  $\text{InO}_4$  distorted tetrahedra. The Rietveld analysis of  $(\text{Ba}_{0.8}\text{La}_{0.2})_2\text{In}_2\text{O}_{5.2}$  confirmed that the  $(\text{Ba}_{0.8}\text{La}_{0.2})_2\text{In}_2\text{O}_{5.2}$  belongs to orthorhombic *Pm3m* space group (Uchimoto *et al.*, 2000). This result indicates that the oxide ion vacancies distribute randomly in the cubic perovskite type structure.

Fig. 1 shows  $k^3$ -weighted In K-edge EXAFS spectra of  $(\text{Ba}_{1-x}\text{La}_x)_2\text{In}_2\text{O}_{5+x}$  ( $X=0.00, 0.10, 0.20, 0.30, 0.40, 0.50$ ). Noise level of these EXAFS spectra seems to be high. The EXAFS spectra of  $(\text{Ba}_{1-x}\text{La}_x)_2\text{In}_2\text{O}_{5+x}$  ( $X=0.00, 0.10, 0.20, 0.30, 0.40, 0.50$ ) exhibited almost the same patterns.

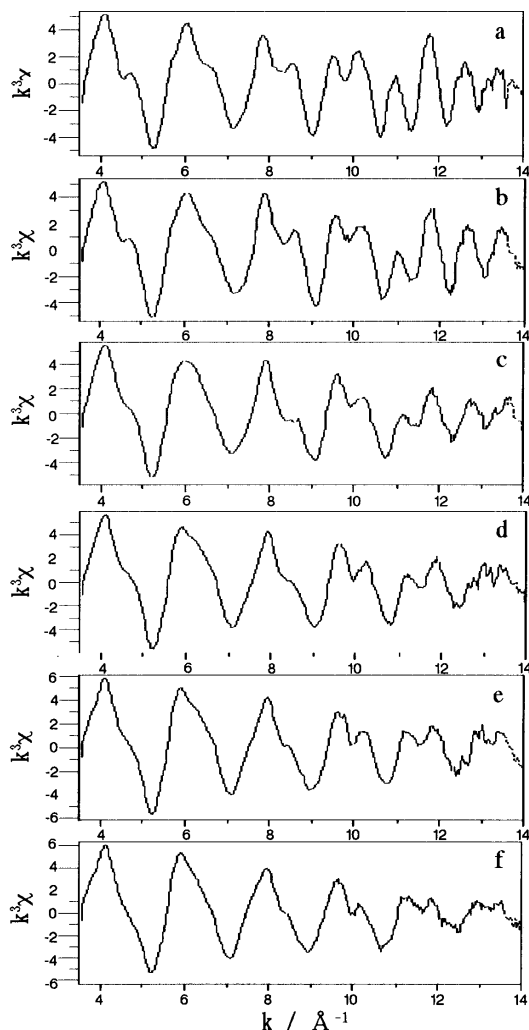


**Figure 1.**  $k^3$ -weighted In K-edge EXAFS spectra of  $(\text{Ba}_{1-x}\text{La}_x)_2\text{In}_2\text{O}_{5+x}$ . X = a: 0.00, b: 0.10, c: 0.20, d: 0.30, e: 0.40, f: 0.50

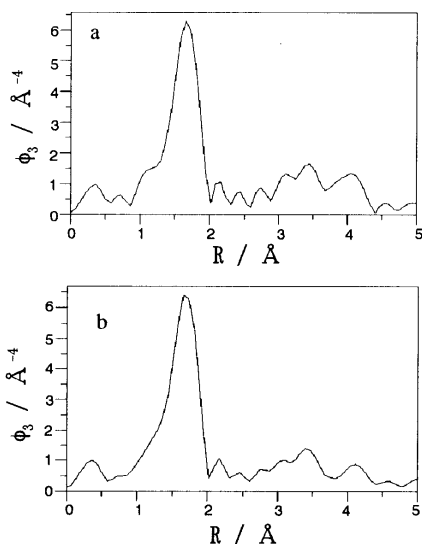


**Figure 2.** Fourier transform of the EXAFS function in the 3.5–14  $\text{\AA}^{-1}$  region of  $(\text{Ba}_{1-x}\text{La}_x)_2\text{In}_2\text{O}_{5+x}$  for the In K-edge. X = a: 0.30, b: 0.50

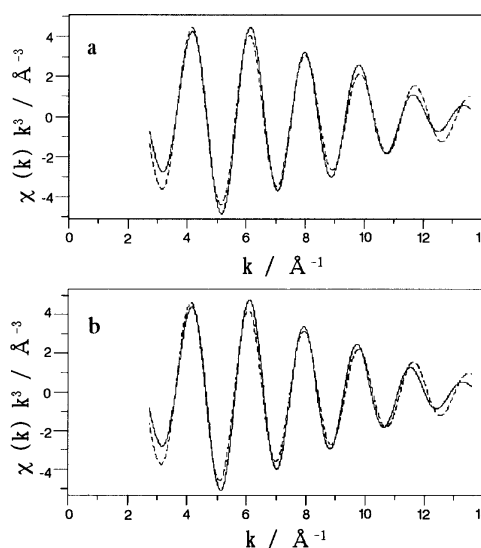


**Figure 3.** Results of the parameter fitting of the EXAFS function of  $(\text{Ba}_{1-x}\text{La}_x)_2\text{In}_2\text{O}_{5+x}$  for the In K-edge. The solid and broken lines present the experimental and calculation, respectively. X = a: 0.30, b: 0.50

Fig. 2 shows Fourier transform data of In K-edge EXAFS of  $(\text{Ba}_{0.7}\text{La}_{0.3})_2\text{In}_2\text{O}_{5.3}$  and  $(\text{Ba}_{0.5}\text{La}_{0.5})_2\text{In}_2\text{O}_{5.5}$ . The peak at  $\sim 1.6 \text{ \AA}$  is attributed to the nearest oxide ion around the  $\text{In}^{3+}$  cation. The oxide ion from both the octahedral and the tetrahedral sites contributes to this peak. In order to analyze the coordination number of  $\text{In}^{3+}$  cation, the peak between 1.2 and 2.0  $\text{ \AA}$  was back-Fourier transformed.

EXAFS function  $\chi(k)$  can be expressed as

$$\chi(k) = \frac{N}{kR^2} |f_0(k)| \exp(-2\sigma^2 k^2) \exp(-2R/\lambda) \sin(2kR + \delta(k))$$

where  $\chi(k)$  is the EXAFS function attributed to the  $\text{In}^{3+}$  ions,  $k$  is the wave vector of the photoelectron,  $f_0(k)$  is the backscattering amplitude of the oxide ion,  $R$  is the distance from  $\text{In}^{3+}$  cation to the oxide ion,  $\sigma^2$  is the variance in the distance  $R$ ,  $\lambda$  is the mean free path of photoelectron, and  $\delta$  is the phase shift. The average coordination number of oxide ion around  $\text{In}^{3+}$  cations is represented by parameter  $N$ . Figure 3 shows the experimental (solid line) and the calculated (dashed line) EXAFS function of  $(\text{Ba}_{0.7}\text{La}_{0.3})_2\text{In}_2\text{O}_{5.3}$  and  $(\text{Ba}_{0.5}\text{La}_{0.5})_2\text{In}_2\text{O}_{5.5}$ .

In the fitting procedure, the ab initio calculated value was used for the backscattering amplitude. (Makale *et al.*, 1988) The values of phase shift  $\delta$  was corrected by using  $\text{Ba}_2\text{In}_2\text{O}_5$  as the standard assuming the coordination number  $N$  is 5.0. The average coordination number of oxide ion around  $\text{In}^{3+}$  cations in  $(\text{Ba}_{1-x}\text{La}_x)_2\text{In}_2\text{O}_{5+x}$  were calculated to give the least-squares fit between the experimental and calculated values of  $c(k)$ . Table 1 shows the curve fitting results of  $(\text{Ba}_{1-x}\text{La}_x)_2\text{In}_2\text{O}_{5+x}$  samples.  $R_{\text{wp}}$  values of  $(\text{Ba}_{1-x}\text{La}_x)_2\text{In}_2\text{O}_{5+x}$  ( $X = 0.00, 0.10, 0.30, 0.40, 0.50$ ), which is

$$\text{calculated by equation, } R_{\text{wp}} = \left| \frac{\sum \{Y_{\text{obs}} - Y_{\text{calc}}\}^2}{\sum (Y_{\text{obs}})^2} \right|^{1/2}, \text{ are } 0.15, 0.17,$$

0.19, 0.17, and 0.18, respectively. This result indicates that the coordination number of  $\text{In}^{3+}$  cation increase with increasing  $\text{La}^{3+}$  cation content. This means oxygen is introduced at interstitial site by keeping an electroneutrality.

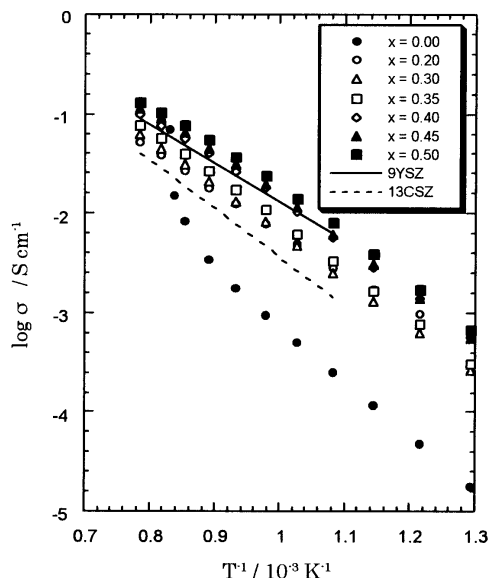


**Figure 4.** Temperature dependence of electrical conductivity of  $(\text{Ba}_{1-x}\text{La}_x)_2\text{In}_2\text{O}_{5+x}$  together with 9YSZ (9 mol%  $\text{Y}_2\text{O}_3$  doped  $\text{ZrO}_2$ ) and 13CSZ (13 mol%  $\text{CaO}$  doped  $\text{ZrO}_2$ ).

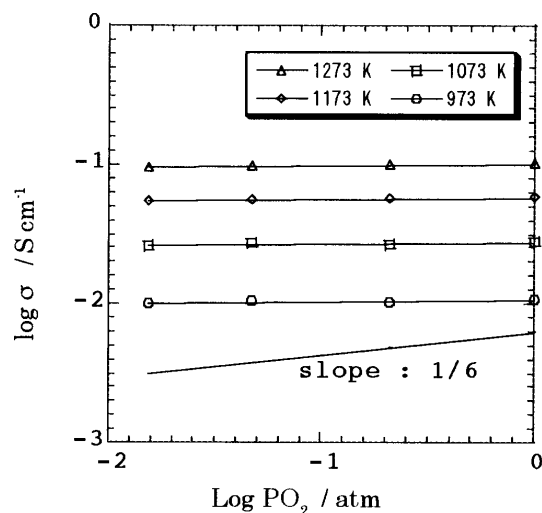
Figure 4 shows electrical conductivities of  $(\text{Ba}_{1-x}\text{La}_x)_2\text{In}_2\text{O}_{5+x}$ . For pure  $\text{Ba}_2\text{In}_2\text{O}_5$ , electrical conductivity rapidly increased above 1203 K due to the order-disorder transition of oxygen vacancy. The electrical conductivities of  $(\text{Ba}_{1-x}\text{La}_x)_2\text{In}_2\text{O}_{5+x}$  ( $x=0.20, 0.30, 0.35, 0.40, 0.45, 0.50$ ) did not show a sharp discontinuity in the conductivity because the disorder phase of defective perovskite type structure was stabilized by doping  $\text{La}^{3+}$  cations at A-site even at low temperature. The conductivity of  $(\text{Ba}_{1-x}\text{La}_x)_2\text{In}_2\text{O}_{5+x}$  ( $x=0.40, 0.45, 0.50$ ) is higher than that of calcia- and yttria-stabilized zirconia.

Fig. 5 shows oxygen partial pressure dependence of electrical conductivity of  $(\text{Ba}_{0.6}\text{La}_{0.4})_2\text{In}_2\text{O}_{5.4}$  at various temperatures. This figure indicates the electrical conductivity is independent of the oxygen partial pressure. The electrical conductivity contains contributions of oxide ion, hole (p-type electronic conduction), and electron (n-type electronic conduction). If the p-type electronic conduction is dominant, the electrical conductivity increased with increasing oxygen partial pressures. Defect equilibrium in  $\text{Ba}_2\text{In}_2\text{O}_5$  was proposed by Zhang et al. (Zhang et al., 1995). They indicated that hole concentration has 1/6 slope against oxygen partial pressure that is in good agreement with the conductivity results of  $\text{Ba}_2\text{In}_2\text{O}_5$  at 873 K. On the other hand, the n-type electronic conduction is dominant, the electrical conductivity decreased with increasing oxygen partial pressures. The result of Fig. 5 indicates that oxide ion transference number is high.

Table 1. Curve fitting results of  $(\text{Ba}_{1-x}\text{La}_x)_2\text{In}_2\text{O}_{5+x}$  samples.

sample	$N^a$	$R^b / \text{\AA}$	$\sigma^{c2} / \text{\AA}^2$
$\text{Ba}_2\text{In}_2\text{O}_5$	5.0	2.10	$4.3 \times 10^{-3}$
$(\text{Ba}_{0.9}\text{La}_{0.1})_2\text{In}_2\text{O}_{5+x}$	5.2	2.10	$4.0 \times 10^{-3}$
$(\text{Ba}_{0.8}\text{La}_{0.2})_2\text{In}_2\text{O}_{5+x}$	5.7	2.11	$4.3 \times 10^{-3}$
$(\text{Ba}_{0.7}\text{La}_{0.3})_2\text{In}_2\text{O}_{5+x}$	5.8	2.11	$3.9 \times 10^{-3}$
$(\text{Ba}_{0.6}\text{La}_{0.4})_2\text{In}_2\text{O}_{5+x}$	5.9	2.12	$3.8 \times 10^{-3}$
$(\text{Ba}_{0.5}\text{La}_{0.5})_2\text{In}_2\text{O}_{5+x}$	6.2	2.12	$4.1 \times 10^{-3}$

$N$  = coordination number of oxide ion around  $\text{In}^{3+}$  cations,  
 $R$  = distance from  $\text{In}^{3+}$  cation to the oxide ion,  $\sigma^2$  = Debye-Waller factor.



**Figure 5.** Oxygen partial pressure dependence of electrical conductivity of  $(\text{Ba}_{0.6}\text{La}_{0.4})_2\text{In}_2\text{O}_{5.4}$  at various temperatures

This research has been partially supported by the Japan Society for the Promotion of Science, "Research for the Future" Program, Production- and Utilization-Technology of Hydrogen Aiming at the Hydrogen Energy Society.

#### References

- Adler, S. B., Reimer, J. A., Baltisberger, J., & Werner, U., (1994). *J. Am. Chem. Soc.*, **116**, 675-681.  
 Appleby, A. J., & Foulkes, F. R., (1989). *Fuel Cell Handbook*, Van Nostrand Reinhold, New York.  
 Feng, M., & Goodenough, J.B., (1995). *Mat. Res. Symp. Proc.*, **369**, 333-336.  
 Goodenough, J.B., Ruiz-Diaz, J.E., & Zhen, Y. S., (1990). *Solid State Ionics*, **44**, 21-31.  
 Ishihara, T., Matsuda, M., Takita, Y., (1994). *J. Am. Chem. Soc.*, **116**, 3801-3803.  
 Makale, A.G., Veal, B.W., Paulikas, A.P., Chan, S.K., & Knapp, G.S., (1988) *J. Am. Chem. Soc.*, **110**, 3763-3768.  
 Minh, N. Q., and Takahashi, T., (1995). *Science and Technology of Ceramic Fuel Cells*, Elsevier, Amsterdam.  
 Uchimoto, Y., Yao, T., Takagi, H., Inagaki, T., & Yoshida, H., (2000). *Electrochemistry*, **68**, 531-533.  
 Uchimoto, Y., Kinuhata, M., & Yao, T., (1999). *Jpn. J Appl. Phys.*, **38**, 111-114.  
 Yao, T., Imafuji, O., & Jinno, H., (1991). *J. Am. Ceram. Soc.*, **74**, 314-317.  
 Yao, T., (1993). *Jpn. J. Appl. Phys.*, **32**, 755-757.  
 Zhang, G. B. & Smyth, D. M., (1995). *Solid State Ionics*, **82**, 161-172.